Available online at www.sciencedirect.com
SCIENCE DIRECT
Molecular Immunology 43 (2006) 812–821
Molecular Immunology
www.elsevier.com/locate/molimm

Genetic and fluorescence studies of affinity maturation in related antibodies

Thierry Pauyo [a], Gerard J. Hilinski [a,1], Philip T. Chiu [a,2], David E. Hansen [a], Yoon J. Choi [b], David I. Ratner [b], Nalini Shah-Mahoney [b], Cathrine A. Southern [a,3], Patricia B. O'Hara [a,*]

[a] *Department of Chemistry, Amherst College, Amherst, MA 01002, USA*
[b] *Department of Biology, Amherst College, Amherst, MA 01002, USA*

Received 9 May 2005; accepted 6 July 2005
Available online 30 August 2005

Abstract

Affinity maturation, the process by which an organism's response to infection becomes more specific and more effective over time, occurs after somatic hypermutation of antibody genes in B-cells. This increase in affinity might be a result of the evolution of either specific interactions between antigen and antibody over time (enthalpic factors) or antibody binding site rigidification (entropic factors) or both. Here, monoclonal antibodies, derived from antibodies elicited at different points in the murine immune response after inoculation with the same diketone hapten, have been characterized both genetically and functionally. Though this hapten has previously been shown to produce the catalytic aldolase antibody 38C2, antibodies described here are not catalytic and unlike 38C2, form no covalent enzyme–substrate complex. Thus, they provide a system in which to assess contributions to the evolution of binding affinity. The genes for these non-catalytic antibodies have been sequenced and analyzed both with regard to their relationships to germ line genes, to each other, and to two commercially available catalytic aldolase antibodies. Consequences of particular mutations for antigen binding behavior are discussed. The protein products of these genes have been expressed, purified, and binding properties measured by two complementary techniques: the hapten-induced quenching of the native antibody fluorescence and the changes in the anisotropy of Prodan (6-propionyl-2-(dimethylamino)naphthalene), a fluorescent hapten analogue. Differences in binding affinity are related back to differences in the lengths and amino acid sequences of the complementary determining region 3 (CDR3) binding loop. Taken together with our earlier results on binding site heterogeneity from tryptophan lifetime analysis [Mohan, G.S., Chiu, P.T., Southern, C.A., O'Hara, P.B., 2004. Steady-state and multifrequency phase fluorometry studies of binding site flexibility in related antibodies. J. Phys. Chem. A 108, 7871–7877], affinity appears to be modulated by a combination of entropic and enthalpic factors, and not dominated by one or the other. Because these antibodies are not related to the same germ line gene, however, these results do not provide evidence for the dominance of enthalpy or entropy in evolving binding affinity in this system.

Keywords: Monoclonal antibodies; Germ line genes; Fluorescence quenching; Fluorescence anisotropy

1. Introduction

Antibody molecules provide protection for an organism against foreign substances that might otherwise prove fatal (Cohn, 2002). One feature of an organism's response to infection by these foreign substances is the expression over time of antibodies with increasing specificity for the foreign substance or antigen (Dal Porto et al., 1998). Several hypotheses exist to explain the driving forces that result in the expression of antibodies with greater affinity for antigen in response to

* Corresponding author. Tel.: +1 413 542 2342; fax: +1 413 542 2345.
E-mail address: pbohara@amherst.edu (P.B. O'Hara).
[1] Present address: Department of Chemistry and Chemical Biology, Harvard University, 12 Oxford Street, Cambridge, MA 02138, USA.
[2] Present address: Department of Materials Science and Engineering, Northwestern University, Evanston, IL 60208, USA.
[3] Present address: Department of Chemistry, College of the Holy Cross, Worcester, MA 01610, USA.

0161-5890/$ – see front matter © 2005 Elsevier Ltd. All rights reserved.
doi:10.1016/j.molimm.2005.07.001

repeated exposures to that antigen (Andersson et al., 1998; Schulz and Lerner, 1995). This process, known as affinity maturation, takes place in germinal centers, which are most abundant in regions of lymphatic tissue such as spleen and tonsils. During affinity maturation, the already large repertoire produced from the many combinations of V, D, and J segments, augmented by junctional diversity, is greatly amplified (Adams et al., 2003). This further expansion happens during rapid cell division of the antibody producing B-cells. B-cells expressing tighter-binding antibodies are selected for proliferation. The remaining cells migrate to the margins of the germinal centers, where they undergo apoptosis, thereby removing those genes from the antibody repertoire. Cycles of expansion and compression of the expressed antibody repertoire occur during the course of infection. One germ line gene might be dominant in an early population, but a shift in the repertoire often occurs as affinity maturation selects alternative genes with the potential for better antigen binding.

A practical consequence of affinity maturation is a population of circulating antibodies that may differ from each other in any one point in time, and can differ from one time point to another over the course of an infection. Mutational activity is focused upon amino acids that line the hapten binding pocket in complementarity determining regions 1–3 (CDR1, CDR2, CDR3) of both the light and heavy chains (Goyenechea and Milstein, 1996). Structurally, the polypeptide regions corresponding to these genes are predominantly in loops that bridge the β-strand scaffolds that form the infrastructure of the molecule (Padlan, 1994). Functionally, these loop regions, three from the heavy chain and three from the light chain, work together to form the antigen binding sites. At the molecular level, one ubiquitous feature of these binding sites is the presence of five or six tryptophan (Trp) residues. The quenching of the Trp fluorescence induced by small molecule hapten binding serves as one of our spectroscopic reporters of binding processes. Classic studies done by Berek and Milstein (1987) correlated increased binding affinities as measured by Trp fluorescence quenching with the mutational frequency during the course of affinity maturation in mice immunized with the small molecule hapten *p*-nitro phenol conjugated with a carrier protein.

One proposed mechanism for enhanced binding affinity that accompanies affinity maturation is the progressive loss of conformational heterogeneity that exists in binding sites derived from immature antibodies or those derived from germ line genes (Mundorff et al., 2000; Schulz and Lerner, 1995). Affinity maturation progresses with the introduction of mutations that reduce flexibility and result in a binding site that is pre-conformed to the molecular structure of the antigen (Manivel et al., 2000b). According to this hypothesis, binding sites with relatively low affinity and a broad selectivity in immature germ line antibodies can be characterized as being flexible while mature antibodies with exquisite selectivity and affinities 100–1000-fold higher, are more rigid than their germ line ancestors. The lack of flexibility in the more mature antibodies should reduce the entropic cost when antibody binds the antigen, thereby leading to a higher affinity. Structural analysis of antibodies at various stages in the immune response lends credence to this idea (Li et al., 2003; Wedemayer et al., 1997). It has been shown that it is not necessary for the new amino acids introduced during affinity maturation to make direct contact with the small molecule hapten (Shannon and Mehr, 1999; Sinha et al., 2002). Further support has come from thermodynamic studies of series of related antibodies using isothermal calorimetry (Furukawa et al., 1999) and surface plasmon resonance spectroscopy (Manivel et al., 2000a). Our earlier work on the same set of antibodies described here showed a narrowing of fluorescence lifetime distributions as the antibodies mature (Mohan et al., 2004), a result consistent with a model in which conformational heterogeneity in the antibody binding site is lost during affinity maturation.

The growing number of results supporting the hypothesis that binding site rigidification accompanies affinity maturation has led us to examine closely the genetic and biophysical properties of antibodies to the diketone hapten shown in Fig. 1a (Turner et al., 2000). Though this hapten elicited the catalytic antibody, 38C2 (Wagner et al., 1995) and a structurally similar hapten elicited catalytic antibody 84G3(Sinha et al., 1999), none of the antibodies produced here shows catalytic function. The four non-catalytic antibodies characterized are derived from animals exposed once (antibody A3.1.1), twice (antibodies 2c26.1 and 2c22.1), or three times (antibody 3.22) to the hapten. As such, they represent different stages of the immune response. Some of these antibodies have been isolated at the moment in which the germinal center activity responsible for expansion of the repertoire is at its highest.

We first determined the V region nucleotide sequences of the four related antibodies. Here, we consider the corresponding polypeptide sequences of the CDR3 region of the heavy chain in detail. Evolutionary relationships between these genes and the germ line genes to which they are related are also discussed. Next, the functional binding behavior of the four monoclonal antibodies (and for comparison the two catalytic antibodies) is characterized using two

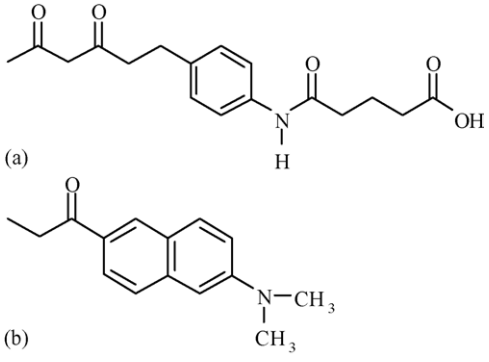

Fig. 1. Chemical structures of (a) the diketone hapten used to elicit aldolase antibody 38C2 and (b) the fluorescent hapten analogue, 6-propionyl-2-(dimethylamino)naphthalene (Prodan).

steady-state fluorescence techniques. In one set of experiments, the hapten-induced fluorescence quenching of native Trp residues is used to determine relative binding affinities for each of the six purified antibodies (Tetin and Hazlett, 2000). In another set of experiments, the binding properties of the different antibodies for Prodan (Weber and Farris, 1979), a highly fluorescent hapten analogue shown in Fig. 1b, are examined. Spectral shifts have been reported for the reversible binding of Prodan to 38C2 antibody (List et al., 1998). Here, we use these spectral shifts and the changes induced in the polarization of Prodan upon binding as a second measure of binding affinity.

2. Experimental

2.1. Materials

The catalytic antibodies 38C2 (#47995-0, Sigma–Aldrich, St. Louis, MO) and 84G3 (#52785-8, Sigma–Aldrich) were purchased and used without further purification. Four of the monoclonal antibodies were produced by the following methodology. Antibodies were elicited in mice injected with the hapten shown in Fig. 1a conjugated to a carrier protein by standard immunological methods (Rose et al., 1997). Animals were sacrificed either 12 days after the initial exposure to the hapten (primary A3.1.1), 5 days after the first boost (secondary antibodies 2c26.1 and 2c22.1), or 5 days after the second boost (tertiary 3.22) and antibody producing cells were isolated from the spleen. Tight-binding populations were selected and standard hybridoma technology was used to create immortal cell lines, which could at any time be injected into the peritoneal cavity of a mouse to produce antibody-secreting tumors. Ascites fluid from the animals was purified using the column and buffers in an ImmunoPure (A/G) IgG Purification Kit (#44902, Pierce Biotechnology, Rockford, IL). Purified antibody was concentrated in a Centricon YM-100 centrifical filtration device (#4213, Millipore Corp., Billerica, MA). Protein purity was confirmed by gel electrophoresis. Catalytic activity of the commercially available antibodies was confirmed by spectroscopic and kinetic studies (data not shown). A non-specific antibody from mouse (#M-9269, Sigma–Aldrich; Mouse IgG1, MOPC 21) was used to test for non-specific interactions of the antibody with the hapten. All solutions were made in phosphate buffered saline (PBS) of 0.010 M Na_2HPO_4, 0.002 M KH_2PO_4, 0.144 M NaCl, 0.003 M KCl, and adjusted to pH 7.2. In every case, this solution was filtered before use with a 0.2 μm Acrodisc® filter (#28143-997, V.W.R. West Chester, PA).

The hapten was synthesized according to published protocol (Wagner et al., 1995). A stock solution of the hapten was made by dissolving 3.0 mg of the hapten in 100 μl of acetonitrile Optima® grade, Fisher Chemicals), and then diluting 1:1250 in filtered PBS to create a 50 μM hapten stock solution that was then added to the antibody solutions. The concentration of a stock solution of hapten was determined by titration with solutions of antibody 38C2 of known concentrations and assuming stoichiometric binding. Prodan (6-propionyl-2-(dimethylamino)naphthalene) (#P248, Molecular Probes, Eugene, OR) stock solutions were prepared by dissolving 4.55 mg of Prodan in 20.0 ml of methanol (Optima® Grade, Fisher Chemicals) resulting in a 100 μM stock solution. The stock solution was kept at −4 °C and protected from light. For optical studies, the stock solution was diluted 1:1000 in filtered PBS to create a 0.1 μM Prodan solution.

2.2. Methods

2.2.1. Sequence analysis

RNA was isolated from ELISA-positive hybridoma cell lines growing in culture using Ultraspec™ reagent (Biotex, Houston, TX). cDNA was prepared with M-MLV reverse transcriptase (Moloney, Murine Leukemia Virus, Gibco-BRL). Expressed antibody heavy and light chain V genes were then amplified using Taq (Takara) DNA polymerase, constant region primers, and degenerate primers derived from the initial nucleotides of the framework 1 region (Wang et al., 2000). The PCR products of separate heavy and light amplifications were gel extracted using the QIAquick Gel Extraction kit (Qiagen, Valencia, CA). In one case, the light chain of 2c.26.1, it was necessary before sequencing to clone the PCR product; pCR2.1 vector (Invitrogen, San Diego, CA) and DH5α cells were used for this purpose. DNA was sequenced by the Biotechnology Resource Center at Cornell University. Presumptive germ line genes were determined by homology searches run at IMGT (http://www.imgt.cines.fr/), NCBI (http://www.ncbi.nlm.nih.gov/igblast/) or using a local, composite collection. Computations of the extent of somatic hypermutation within V and alignments of different V regions, made use of Lasergene software. To assure reproducibility and avoid PCR-generated mutation, cells from each of the monoclonal lines were analyzed in duplicate. Full DNA sequences are available upon request.

2.2.2. Tryptophan fluorescence quenching studies

For each antibody studied, protein concentrations were measured in a 1 ml quartz cuvette by UV–vis spectroscopy (Perkin-Elmer Lambda 2) using the absorption at 280 nm ($\varepsilon_{280} = 1.35\,(\mathrm{mg/ml})^{-1}\,\mathrm{cm}^{-1}$). Steady-state excitation and emission spectra were collected using either a K2 multifrequency phase fluorometer (ISS, Champagne-Urbana, IL) or an LS50B fluorimeter (Perkin-Elmer, Boston, MA). Excitation spectra were recorded by monitoring the fluorescence signal at the emission maximum (approximately 335 nm) while scanning the excitation wavelength. For the ISS K2 measurements, a Xenon arc lamp set at a current of 10 A was used as the excitation source; a monochromator with a dispersion of 8 nm/mm was used to select the excitation frequency. The emission spectra were recorded by exciting the solution at 284 nm and collecting the fluorescence signal through a monochromator with a dispersion of 8 nm/mm. The slitwidths of both the excitation and emission

monochromators were 0.5 mm in all cases. For the LS50B experiments, slit widths of 5 nm for both the excitation and emission monochromators were used. For both instruments, the temperature of the solutions was maintained at 20 °C using a re-circulating water bath. A spectrum of the antibody solution with no hapten was acquired first, then successive additions of hapten solution were made and fluorescence collected after each addition, until the concentration of hapten exceeded the concentration of antibody binding sites. Antibody concentrations varied from 0.15 to 7.8 μM. After each addition of hapten the solution was mixed, and then allowed to equilibrate at 20 °C for 2 min before the emission spectrum was acquired.

The value of the antibody-hapten dissociation constant can be determined from tryptophan quenching data because the amount of quenching observed is related to the fraction of antibody binding sites filled (F_b) according to the following relationship:

$$F_b = \frac{F_0 - F}{F_0 - F_{mq}} \quad (1)$$

where F_0 is the tryptophan fluorescence intensity (at the emission maximum, 335 nm) in the absence of hapten, F the tryptophan fluorescence intensity observed in the presence of hapten, and F_{mq} is the tryptophan fluorescence intensity with maximum quenching. In all cases, the values of F were corrected for dilution effects prior to analysis. The value of F_{mq} is expected to be non-zero for these studies because many of the tryptophan residues in antibodies are not located at the binding sites, and the fluorescence from these residues should not be quenched as a result of hapten binding. A plot of $F_0 - F$ versus the total hapten concentration (L_t) can be used to determine the value of K_d for the antibodies studied based on the following expression:

$$F_0 - F = (F_0 - F_{mq})\frac{(K_d + S_t + L_t) - \sqrt{K_d^2 + 2K_dS_t + 2K_dL_t + S_t^2 - 2S_tL_t + L_t^2}}{2S_t} \quad (2)$$

where S_t is the total concentration of antibody binding sites, and all other parameters are defined above. This expression was used to fit plots of $F_0 - F$, with both K_d and F_{mq} as fitting parameters, using the Igor Pro (Wavemetrics, Lake Oswego, OR) software package. This type of analysis has been used previously for the determination of antibody-hapten dissociation constants (Tetin and Hazlett, 2000).

2.2.3. Prodan steady-state fluorescence and fluorescence anisotropy studies

Prodan concentrations were measured in 3 mm × 3 mm × 43 mm quartz cuvettes by UV–vis spectroscopy using a Lambda 2 (Perkin-Elmer) using the absorption at 361 nm (ε_{361} = 18,000 cm^{-1} M^{-1}). Prodan steady-state fluorescence spectra were acquired using an LS50B luminescence spectrometer (Perkin-Elmer). For these measurements, the slit width of the excitation and emission monochromators was 5 nm. The temperature of the solutions was maintained at 20 °C using a re-circulating water bath.

Fluorescence anisotropy measurements of Prodan were carried out using a Beacon 2000 polarimeter (Invitrogen, Carlsbad, CA). A band pass filter with a central transmission wavelength of 360 nm was used to select the appropriate excitation wavelength for Prodan. The emission filter used for the anisotropy measurements has a central transmission wavelength of 490 nm and a band pass of 10 nm. This filter was chosen because it transmits in a wavelength region where the fluorescence quantum yields of bound and free Prodan are approximately equal (see Fig. 3). A solution of Prodan (either 20 or 100 nM) was examined initially, and then successive additions of antibody were made until the total concentration of antibody binding sites was ≈2 μM. After each addition, the solution was vortexed and allowed to equilibrate for 5 min before measuring the anisotropy. For each addition, 10 successive measurements of the fluorescence anisotropy were acquired, and then averaged before plotting.

Because the fluorescence anisotropy of Prodan is linearly related to the fraction of antibody binding sites filled, measurements of this parameter as a function of the concentration of free antibody binding sites allows the antibody-Prodan dissociation constant to be determined according to the following relationship:

$$A = \frac{(A_{max} - A_{min})[S]}{K_d + [S]} + A_{min} \quad (3)$$

where A is the fluorescence anisotropy, A_{max} the maximum anisotropy observed, A_{min} the minimum anisotropy observed, and $[S]$ is the concentration of free antibody binding sites. The concentration of free antibody binding sites was approximated by the total concentration of antibody binding sites, which is a valid approximation as long as the concentration of Prodan used is at least 10-fold lower than the observed K_d values. The concentration of Prodan varied with the antibody studied, but in all cases the concentration used satisfied this condition. Plots of anisotropy versus the concentration of antibody binding sties were fit according to Eq. (3) using Igor Pro software (Wavemetrics, Lake Oswego, OR), with A_{max}, A_{min}, and K_d as fitting parameters.

3. Results

3.1. Sequence analysis of CDR3

The amino acid sequences of the heavy chain CDR3 for the six antibodies are shown in Table 1. The beginning of CDR3, the hypervariable loop bridging the β strands of framework region 3 (FR3) and framework region 4 (FR4), is marked by

Table 1
Amino acid sequences of CDR3 in related antibodies

Monoclonal Antibody [a]	Shown is a portion of the heavy chain amino acid sequence at CDR3 starting with conserved Y at **H**90			Source
84G3 heavy	YY	**CAKHTYGGPG----------DSW**	GQ [b]	Sigma Aldrich
38C2	YY	**CKTYFYSFS----------YW**	GQ [b,c]	Sigma Aldrich
3.22	YY	**CIRGGTAYNRYDG------AYW**	GQ	Tertiary/5 day
2c26.1	YY	**CATAHYVNPGRFTKTLDYW**	GQ	Secondary/5 day
2c22.1	YY	**CTRGNYGYVG----------AYW**	GQ	Secondary/5 day
A 3.1.1	YY	**CTRWGY----------AYW**	GQ	Primary/12 day

[a] Light chain, class κ; heavy chain class G or G_1.
[b] Sequences for 84G3 and 38C2 are from Zhu et al., 2004 *J.M B.* **343** 1269-1280.
[c] Catalytic lysine for 38C2 is underlined.

a conserved cysteine at position H92. The terminus of the loop is marked by a conserved Trp. The sequence for each heavy chain CDR3 includes at least one basic side group. Acid side groups are scarce. Five of the six antibodies have lysine (Lys) or arginine (Arg) in the second (H93) or third (H94) position in CDR3. Primary A3.1.1, secondary 2c22.1 and tertiary 3.22 all have Arg at position H94. Secondary 2c26.1 has three basic residues further along in the sequence. Five of the six sequences have tyrosine (Tyr) in position H97. The exception, tertiary 3.22, will be shown to have the lowest binding affinity. The CDR3 of primary A3.1.1 also contains an extra tryptophan (Trp) residue in the combining site, which has potentially significant effects for the fluorescence behavior. The lengths of CDR3 vary considerably, from 9 amino acids in primary A3.1.1 to 19 amino acids in secondary 2c26.1.

For the catalytic antibody 38C2, this loop is 11 amino acids in length and contains the catalytic Lys residue at position H93. This Lys, with its extremely low pK_a, acts as the nucleophile to form the Schiff base linkage with the substrate in the first step of the aldolase reaction, which it catalyzes (Wagner et al., 1995). To date, catalytically active aldolase antibodies have fallen into two classes as distinguished by the enantiomeric selectivity of their reactions. The structures of catalytic antibodies 33F12 (similar in sequence and reactivity to 38C2) and 93F3 (similar in sequence and reactivity to 84G3) have recently been solved (Zhu et al., 2004). By analogy to its position in the structurally similar antibody 33F12, Lys H93 in 38C2 has been shown to be located at the bottom of a 10 Å deep pocket into which the hapten binds. It is surrounded by hydrophobic residues, which explains its extremely low pK_a. Catalytic antibody 84G3 has alanine, not Lys, at position H93. By analogy to its structurally similar 93F3, the Lys at H94 of 84G3 points away from the binding pocket, and thus cannot act as the catalytic nucleophile. Instead, Lys L89 on the light chain points directly into the other side of the pocket, explaining the differential antipodal selectivities of the two classes of catalytic antibodies. None of our monoclonal antibodies raised in mice by reactive immunization against the same diketone hapten used to elicit 38C2, contains a Lys at position H93 or L89, and none assayed to date has shown catalytic activity.

The "evolutionary" relationship of the genetic sequences of the V regions of the heavy chain genes of the six antibodies can be estimated. The vast diversity available in the germ line antibodies comes partly from different combinations of the germ line genes for the V region (corresponding to approximately the first 90 residues), with the 13 different germ line genes for the D region (corresponding to hypervariable region) and the 4 different germ line genes for the J region (corresponding to the remaining 15 residues) (Goldsby et al., 2003). The hypervariable CDR3 loop responsible for the binding of the hapten is created through two joining events, D to J and then V to DJ. Beyond the given diversity of the germ line, junctional diversity and somatic hypermutation produce mutations, deletions, and insertions that result in mature antibodies with enhanced binding selectivity and affinity. Table 2 reports the percent identity of amino acids in the V region of the heavy chain for the six antibodies. The highest identity, 76%, is exhibited between the heavy chains for A3.1.1 and

Table 2
Percent identity in V region of heavy chain in antibodies[a]

	84G3 mature	38C2 mature	3.22 tertiary	2c26.1 secondary	2c22.1 secondary	A3.1.1 primary
84G3	×	44.1	70.5	57.1	40.2	41.1
38C2		×	44.1	41.4	46.8	48.6
3.22			×	52.5	49.6	49.6
2c26.1				×	46.2	47.9
2c22.1					×	76.1
A3.1.1						×

[a] The pairwise extent of amino acid identity excludes residues corresponding to the degenerate PCR primer at the start of FR1, but includes the contributions of D and J genes. Alignments relied upon the ClustalW algorithm.

2c22.1. The remainder of our antibodies hovers in the range of 45–50% identity. At least five different germ line genes gave rise to these six antibodies, all of which bind tightly to diketone hapten. It is notable that five of these six antibodies were raised against the same diketone hapten.

Table 3 lists the number of nucleotide mutations in the V region of the five antibodies raised against the same diketone hapten relative to the closest aligning germ line sequence for both heavy and light chains. It is important to note that, in contrast to the murine light chain genes, the public databanks do not yet include all genes encoding the heavy chains of mouse antibodies. In fact, the three databases used here, NCBI, IMGT, and our own composite, sometimes give the same germ line reference and sometimes not. Since the closest aligning germ line sequence, taken to be the gene from which a given antibody has derived, may simply not yet be available, the number of heavy chain nucleotide mutations may be over-stated. The germ line sequence that aligns best is assumed to be the germ line predecessor of that DNA sequence. Any differences between the two sequences are the result of somatic hypermutation. Those antibodies that exhibit large numbers of nucleotide mutations relative to the germ line sequence have undergone extensive affinity maturation, and vice versa. The best alignment for 38C2 is obtained from germ line genes that have undergone 13 mutations in the light chain and 25 in the heavy chain. It is interesting to note that secondary 2c26.1 and tertiary 3.22 are derived from the same germ line light chain gene D00081.

Table 3
Antibody alignment to germline sequences in the IMGT database[a]

Antibody		Closest IMGT aligning germ line sequence	Number of nucleotide mutations in V region
84G3 (tertiary)	Light chain	No data available	
	Heavy chain		
38C2 (tertiary)	Light chain	D00080	13
	Heavy chain	X03398	25
3.22 (tertiary)	Light chain	D00081	1
	Heavy chain	U53526	18
2c26.1 (secondary)	Light chain	D00081	2
	Heavy chain	AJ223544	14
2c22.1 (secondary)	Light chain	AJ231217	22
	Heavy chain	D14633	12
A 3.1.1 (primary)	Light chain	Y15976	0
	Heavy chain	AF304547	11

[a] The number of somatic mutations tabulated excludes regions corresponding to the D or J segments, and also excludes the FR1 region corresponding to our degenerate primers.

Berek and Milstein demonstrated that for antibodies specific for the V_κ-Ox1 germline gene, which dominates the response against 2-phenyl-5-oxazolone (phOx) hapten, the average numbers of light chain nucleotide mutations for a primary 14 days, a secondary, and a tertiary antibody are 3, 5.9, and 7.3, respectively (Berek and Milstein, 1987). Binding affinity for hapten generally correlated with an increase in the number of mutations (though the correlation is far from absolute). By contrast, the number of nucleotide mutations in the variable region of the light chain fluctuates from the primary to the secondary to the tertiary in the monoclonal antibodies described here. Since nucleotide mutations can be random and not necessarily related to an increase in the binding affinity of the antibody, it is important to measure the binding constants of A3.1.1, 2c26.1, 2c22.1, and 3.22 directly.

3.2. Tryptophan fluorescence quenching measurements

Fig. 2a shows the quenching of the Trp fluorescence induced by binding hapten. The residual fluorescence observed at 340 nm at saturating conditions of hapten derives from Trp residues that are far from the binding site. All of the monoclonal antibodies under investigation possess a total of 24–28 Trp residues, only 10–12 of which are close to the binding sites (Wang et al., 2000). Precise numbers for binding site versus total Trp for the six antibodies under investigation are: 12/24, 10/24, 10/26, 10/26, 10/26, and 12/28 for 84G3, 38C2, tertiary 3.22, secondary 2c26.1, secondary 2c22.1, and primary A3.1.1, respectively.

Fig. 2b shows the fits of the data using Eq. (2) for five of the six antibodies in this study. Table 4 reports the dissociation constants derived from this quenching data using Eq. (2). Binding to the four monoclonal antibodies from our library is not covalent as determined experimentally by the lack of catalytic activity, the absence of a spectroscopic signature

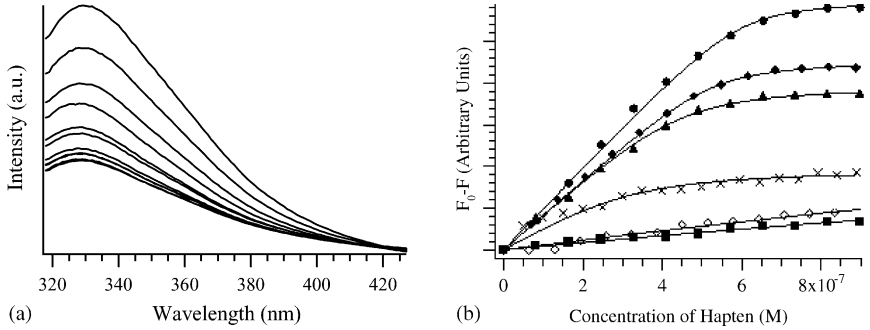

Fig. 2. Tryptophan emission spectra observed for 38C2 at 2.22 μM (≈0.5 mg/ml) antibody in a PBS solution of 0.010 M Na_2HPO_4, 0.002 M KH_2PO_4, 0.144 M NaCl, 0.003 M KCl, pH 7.2. Panel a: quenching of Trp fluorescence observed upon addition of hapten in 2 μl increments from a 50 μM stock solution in PBS. The spectra shown have not been corrected for dilution factors. Excitation wavelength is 284 nm. Panel b: plots of $F_0 - F$ vs. hapten concentration for the following antibodies: 38C2 (●), 84G3 (♦), secondary 2c26.1(▲), secondary 2c22.1 (×), primary A3.1.1 (■), and IgG1 (MOPC 21) (◊). F is the Trp fluorescence intensity observed and F_0 is the Trp fluorescence intensity observed in the absence of hapten. The data were fit using Eq. (2). The values of K_d obtained from the fits are presented in Table 4.

of the vinylogous amide derived from the hapten-antibody adduct and the lack of an active site Lys in position H93 as shown in Table 1 or L89 (data not shown).

Binding of the hapten to both catalytic antibodies is stoichiometric, fits of the data to Eq. (2) yield dissociation constants of 9.02 ± 3.16 nM for 38C2 and 11.8 ± 1.15 nM for 84G3. This number is only used as a test of the lower limit of our technique since binding to these two antibodies should be irreversible and covalent. The four monoclonal non-catalytic antibodies reveal binding affinities that vary from strong for secondary antibodies 2c26.1 and 2c22.1 (K_d = 0.023 and 0.051 μM) to weak for primary A3.1.1 (K_d = 5.46 μM) to very weak (K_d = 25.4 μM) for tertiary 3.22. The binding affinities for hapten vary by a factor of 3000 for antibodies raised against the same hapten. Given that 84G3 was raised against a similar but not identical hapten, it is surprising that it binds this hapten as tightly as it does, but two things must be noted. First, as stated earlier, the binding constants of the two catalytic antibodies are somewhat fictitious in that the binding is irreversible and these low K_d values of ∼10 nM set a lower limit to K_ds that can be measured using the Trp quenching technique under these conditions. The second is that 84G3 has an additional Trp at the binding site, and it is not totally clear how this will affect the binding constant measured using Trp quenching.

3.3. Prodan fluorescence anisotropy measurements

All chemical and physical evidence is consistent with a model in which binding of Prodan to any of the antibodies studied here (including catalytic 38C2 and 84G3) is reversible and not covalent. As such, Prodan serves as another indicator of relative binding affinity for all the antibodies in this analysis. Previous studies have also noted a variation in the Stokes shift of Prodan when bound to various biomolecules (List et al., 1998; Mohan et al., 2004). Increased Stokes shifts (red shift in the emission) for Prodan have been interpreted as indicating decreased hydrophobicity of binding sites. Fig. 3a shows the 528 nm emission max for Prodan in PBS shifts to 450 nm upon binding to antibody 38C2. Introduction of non-specific IgG results in an emission maximum identical to that observed for unbound Prodan, and no increase in the anisotropy, suggesting that Prodan does not bind to non-specific IgG data not shown).

As shown in Fig. 3b, the anisotropy measured at 487 nm rises as the Prodan is titrated with each member of the antibody family under analysis. The measured anisotropy for the Prodan varies from ∼60 mA in solution to a maximum value of ∼300 mA when bound to the six antibodies shown here. Fits of Eq. (3) to the data are shown by the curves in Fig. 3b. Table 4 tabulates the dissociation constants derived from the

Table 4
Dissociation constants as determined for hapten from Eq. (2) and for Prodan from Eq. (3)

Antibody	K_d hapten Trp quenching	$K'_d/K_{dq(38C2)}$ hapten Trp quenching	K_d Prodan anisotropy (μM)	$K_d/K_{d(38C2)}$ Prodan anisotropy
38C2 mature	9.03 ± 3.16 nM[a]	1	0.48 ± 0.06	1
84G3 mature	11.8 ± 1.15 nM[a]	1.31	0.122 ± 0.005	0.26
3.22 tertiary	25.4 ± 6.8 μM	2813	1.6 ± 0.1	3.3
2C26.1 secondary	0.023 ± 0.006 μM	2.55	2.1 ± 0.5	4.4
2c22.1 secondary	0.051 ± 0.025 μM	5.65	1.3 ± 0.2	2.7
A3.1.1 primary	5.46 ± 2.57 μM	605	0.8 ± 0.2	1.7
Control IgG[b]	7.26 ± 5.25 μM	804	>100	>1000

[a] Antibodies 84G3 and 38C2 show irreversible tight binding to the hapten due to active site lysines which react with the diketone to form a Shiff base adduct. This binding is technically stoichiometric.
[b] Control IgG was a non-specific murine IgG1, Kappa (MOPC 21).

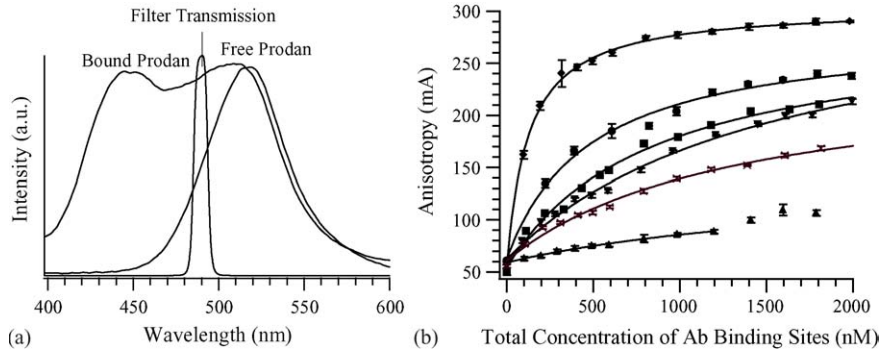

Fig. 3. Emission spectra of 20 nM Prodan excited at 375 nm shifts as a function of successive additions of antibody 38C2. Panel a: an isosbectic point occurs at approximately 487 nm. Polarization collected at this wavelength through the filter shown contains contributions from both free and bound Prodan and can be used to calculate binding constants. Panel b: plots of Prodan fluorescence anisotropy vs. the total concentration of antibody binding sites for the following antibodies: 38C2 (●), 84G3 (♦), tertiary 3.22 (▼), secondary 2c26.1 (▲), secondary 2c22.1 (×), and primary A3.1.1 (■) antibodies. The anisotropy was measured at 490 nm, where both free and bound Prodan fluoresce with nearly equal fluorescence quantum yields. The data were fit using Eq. (3). The values of K_d obtained from the fits are presented in Table 4.

analysis of this data. Despite the fact that no covalent bond is formed here, the mature catalytic antibodies still show the strongest binding affinities ($K_d = 0.122 \pm 0.005\,\mu M$ for 84G3 and $0.48 \pm 0.06\,\mu M$ for 38C2). Binding of Prodan to primary A3.1.1 proved to be tightest of the non-catalytic clones ($K_d = 0.8 \pm 0.2\,\mu M$) while the binding constant of secondary 2c26.1 proved to be the weakest measured ($K_d = 2.1 \pm 0.5\,\mu M$). Perhaps the most striking characterization of the Prodan binding to the six antibodies is that they all have binding affinities for Prodan that are very similar. The weakest binder 2c26.1 binds Prodan only 6.5 times more weakly than the tightest binder 84G3.

We know the binding of Prodan to the antigen binding site is specific based on the spectra shown in Fig. 4. Addition of antibody to a dilute solution of Prodan shifts the emission spectrum to the blue, as typical of bound Prodan. Subsequent addition of the diketone hapten displaces the Prodan from the active site and the spectrum reverts back to the original spectrum of unbound Prodan. This shows that binding of Prodan is specific, that the hapten and Prodan cannot coexist at the binding site, and that, by inference, the Prodan anisotropy should be a good measure of binding and flexibility of the probe in the antibody binding site.

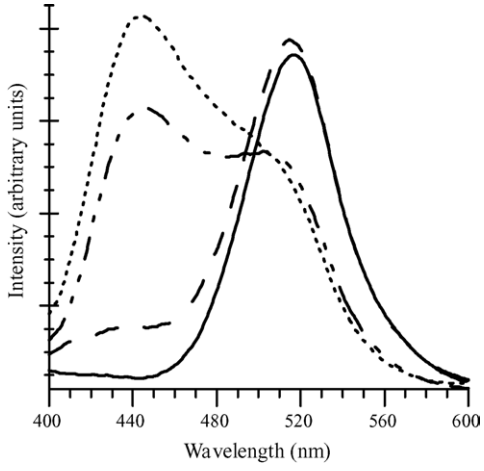

Fig. 4. Emission spectra of a 20 nM aqueous solution of Prodan (—), 20 nM Prodan and 400 nM 38C2 (– – –), 20 nM Prodan and 800 nM 38C2 (- - -), and 20 nM Prodan, 800 nM 38C2, and 800 nM hapten (— —). The fact that the Prodan emission spectrum in the presence of the hapten closely mimics the emission spectrum of free Prodan demonstrates that Prodan binds specifically.

4. Discussion

Affinity maturation might be expected to be accompanied by an increase in the number of mutations from a germ line gene and by tighter binding of the antibody to a small molecule hapten or fluorescent hapten analogue. In our system, mutational frequency does not correlate with the immune response time point at which the antibody was harvested. Antibodies harvested after one, two, or three inoculations show a fairly low mutational rate while another antibody harvested after two inoculations shows a number of mutations similar to the mature antibody 38C2. This irregularity is especially noteworthy for the light chain, for which the complete germ line assemblage is known.

Hapten binding affinities for the primary antibody (A3.1.1) and both secondary antibodies (2c22.1 and 2c26.1) vary in a predictable manner: antibodies harvested later in the immune response bind hapten more tightly. The exception is tertiary antibody 3.22 which appears to be much more like a primary antibody, both in its low mutational rate and its weak affinity for hapten. Comparison of the sequence of the loops with the binding affinity shows that the tightest non-covalent binder (secondary 2c26.1) has the longest CDR3 loop (19 residues) and the greatest number of positively charged side groups. Primary A3.1.1 with the shortest CDR3 loop (9 residues) displays weak binding. The interesting connection between loop size and hapten affinity is made more intriguing when considering previous results (Mohan et al., 2004) which demonstrated that this same antibody, 2c26.1, exhibited the greatest difference in Trp lifetime distributions upon addition

of hapten. Understood now in terms of the length of the CDR3 loop, it makes sense that a large flexible loop would exhibit dynamic flexibility, and that binding of hapten to the loop would reduce that flexibility. By contrast, A3.1.1 was shown to have a much more limited change in Trp lifetime distributions upon binding hapten; with the shorter loop, it pays a lower entropic cost, though this does not result in tighter binding. Taken together, these data suggest that within this panel of non-covalent binding antibodies, enhanced enthalpic factors must be responsible for the greater binding affinity of 2c26.1 and not reduced entropic costs originating from conformational pre-formation. It must be emphasized that these data cannot be used as evidence for or against conformational rigidity (or pre-conformation) of the binding site upon affinity maturation, since a true test of this model must compare properties of antibodies of the same genetic lineage, isolated at various points in the immune response.

Prodan binding results show unequivocally that Prodan displaces hapten and is, therefore, bound specifically at the antigen binding site. Antibodies tested here bound Prodan relatively tightly, though differences in binding affinity were small. It is interesting to note that in contrast to hapten binding, antibodies with the shortest loops exhibited the tightest binding. As the size of CDR3 increases, the binding affinity for Prodan decreases. If binding site rigidification correlates with antibody maturity, one might expect that the values for the limiting anisotropy of a bound fluorescent hapten analogue might increase from primary to secondary to tertiary antibodies. Again, antibodies of the same genetic lineage are necessary to answer this important question. Experiments to measure these properties on a larger set of antibodies are underway.

5. Conclusions

Though this system is too limited to provide us with the data necessary to make over-arching claims about affinity maturation, it has shown us that we must be careful in identifying antibodies harvested after multiple inoculations as mature, as we have shown at least one case in which this is not true. It also reveals the robust nature of the immune response in that each of the antibodies characterized, though elicited against the same antigen, recruited a different heavy chain germ line gene and with one exception, different light chain germ line genes. It has also been shown that in this small set of antibodies, binding affinity is not dominated by either entropic (conformational flexibility) or enthalpic factors, but that each aspect contributes to overall binding affinity.

Acknowledgements

The work would not have been possible without the generosity and guidance of Richard Goldsby, in whose lab the antibodies and the hybridoma cell lines were produced. The following undergraduate students also contributed to this project: Bryan Dolan, Lee Jay Henry, Gopi Mohan, Elise Nguyen, Josephine Nguyen, and Shormeh Yeboah. Elizabeth Radwilowicz, a chemistry teacher at Belchertown High School, made further contributions while working at Amherst College during the summer of 2004. Funding for this work was provided by the National Science Foundation through its Collaborative Research at Undergraduate Institutions Program (Awards 9510212 and 9978779), the Camille and Henry Dreyfus Scholar/Fellow Program for Undergraduate Institutions, and by a grant from the Amherst College Faculty Research Award Program, as funded by the H. Axel Schupf '57 Fund for Intellectual Life.

References

Adams, C.L., Macleod, M.K.L., James Milner-White, E., Aitken, R., Garside, P., Stott, D.I., 2003. Complete analysis of the B-cell response to a protein antigen, from in vivo germinal centre formation to 3-D modelling of affinity maturation. Immunology 108, 274–287.

Andersson, K., Wrammert, J., Leanderson, T., 1998. Affinity selection and repertoire shift: paradoxes as a consequence of somatic mutation? Immunol. Rev. 162, 173–182.

Berek, C., Milstein, C., 1987. Mutation drift and repertoire shift in the maturation of the immune response. Immunol. Rev. 96, 23–41.

Cohn, M., 2002. The immune system: a weapon of mass destruction invented by evolution to even the odds during the war of the DNAs. Immunol. Rev. 185, 24–38.

Dal Porto, J.M., Haberman, A.M., Shlomchik, M.J., Kelsoe, G., 1998. Antigen drives very low affinity B cells to become plasmacytes and enter germinal centers. J. Immunol. 161, 5373–5381.

Furukawa, K., Akasako-Furukawa, A., Shirai, H., Nakamura, H., Azuma, T., 1999. Junctional amino acids determine the maturation pathway of an antibody. Immunity 11, 329–338.

Goldsby, R., Kindt, T.J., Osborne, B., Kuby, J., 2003. Immunology. Freeman.

Goyenechea, B., Milstein, C., 1996. Modifying the sequence of an immunoglobulin V-gene alters the resulting pattern of hypermutaion. Proc. Natl. Acad. Sci. U.S.A. 93, 13979–13984.

Li, Y., Li, H., Yang, F., Smith-Gill, S.J., Mariuzza, R.A., 2003. X-ray snapshots of the maturation of an antibody response to a protein antigen. Nat. Struct. Biol. 10, 482–488.

List, B., Barbas III, C.F., Lerner, R.A., 1998. Aldol sensors for the creation of tunable fluorescence from antibody catalysts. Proc. Natl. Acad. Sci. U.S.A. 95, 15351–15355.

Manivel, V., Sahoo, N.C., Salunke, D.M., Rao, K.V.S., 2000a. Maturation of an antibody response in goverened by modulations in flexibility of the antigen-combining site. Immunity 13, 611–620.

Manivel, V., Sahoo, N.C., Salunke, D.M., Rao, K.V.S., 2000b. Maturation of an antibody response is governed by modulations in flexibility of the antigen-combining site. Immunity 13, 611–620.

Mohan, G.S., Chiu, P.T., Southern, C.A., O'Hara, P.B., 2004. Steady state and multifrequency phase fluorometry studies of binding site flexibility in related antibodies. J. Phys. Chem. A 108, 7871–7877.

Mundorff, E.C., Hanson, M.A., Varvak, A., Ulrich, H., Schultz, P.G., Stevens, R.C., 2000. Conformational effects in biological catalysis: an antibody-catalyzed oxy-cope rearrangement. Biochemistry 39, 627–632.

Padlan, E.A., 1994. Anatomy of the antibody molecule. Mol. Immunol. 31, 169–217.

Rose, N., DeMacrio, E., Fahey, J., Friedman, H., Penn, G., 1997. Manual of Clinical Laboratory Immunology. American Society Microbiology Press, Washington, DC.

Schulz, P.G., Lerner, R.A., 1995. From molecular diversity to catalysis: lessons from the immune system. Science 269, 1835–1842.

Shannon, M., Mehr, R., 1999. Reconciling repertoire shift with affinity maturation: the role of deleterious mutations. J. Immunol. 162, 3950–3956.

Sinha, N., Mohan, S., Lipschultz, C.A., Smith-Gill, S.J., 2002. Differences in electrostatic properties at antibody-antigen binding sites: implications for specificity and cross-reactivity. Biophys. J. 83, 2946–2968.

Sinha, S.C., Sun, J., Miller, G., Barbas III, C.F., Lerner, R.A., 1999. Sets of aldolase antibodies with antipodal reactivities. formal synthesis of epothilone E by large-scale antibody-catalyzed resolution of thiazole aldol. Org. Lett. 1, 1623–1626.

Tetin, S.Y., Hazlett, T.L., 2000. Optical spectroscopy in studies of antibody–hapten interactions. Methods 20, 341–361.

Turner, J.M., Bui, T., Lerner, R.A., Barbas III, C.F., List, B., 2000. An efficient benchtop system for multigram-scale kinetic resolutions using aldolase antibodies. Chem. A Eur. J. 6, 2772–2774.

Wagner, J., Lerner, R.A., Barbas III, C.F., 1995. Efficient aldolase catalytic antibodies that use the enamine mechanism of natural enzymes. Science 270, 1797–1800.

Wang, Z., Raifu, M., Howard, M., Smith, L., Hansen, D., Goldsby, R., Ratner, D., 2000. Universal PCR amplification of mouse immunoglobulin gene variable regions: the design of degenerate primers and an assessment of the effect of DNA polymerase 3′ to 5′ exonuclease activity. J. Immunol. Methods 233, 167–177.

Weber, G., Farris, F.J., 1979. Synthesis and spectral properties of a hydrophobic fluorescenct probe: 6-propionly-2-(dimethylamino)-napthalene. Biochemistry 18, 3075–3078.

Wedemayer, G.J., Patten, P.A., Wang, L.H., Schultz, P.G., Stevens, R.C., 1997. Structural insights into the evolution of an antibody combining site. Science 276, 1665–1669.

Zhu, X., Tanaka, F., Hu, Y., Heine, A., Fuller, R., Zhong, G., Olson, A.J., Lerner, R.A., Barbas III, C.F., Wilson, I.A., 2004. The origin of enantioselectivity in aldolase antibodies: crystal structure, site-directed mutagenesis, and computational analysis. J. Mol. Biol. 343, 1269–1280.